V. Yu. KERIMOV, *Head of Department*[1], *Leading Researcher*[2], *Doctor of Geological Sciences, kerimovvy@mgri.ru*
E. V. VYATKINA[1], *Lecturer*
V. Sh. GURBANOV[2], *Chief Operating Officer, Professor, Doctor of Geological Sciences*
I. S. KOROTCHENYA[3], *Candidate for a Master's Degree*

[1] *Sergo Ordzhonikidze Russian State University for Geological Prospecting, Moscow, Russia*
[2] *Ministry of Science and Education of the Republic of Azerbaijan, Institute of Oil and Gas, Baku, Azerbaijan*
[3] *National University of Science and Technology MISIS, Moscow, Russia*

CRITERIA FOR THE HYDROCARBON POTENTIAL OF SHALE FORMATIONS IN THE SOUTH CASPIAN BASIN

The study presents research findings to prove the shale nature of the Diatom suite, the Maikop series and the Eocene deposits of the South Caspian Basin, which are characterized as hybrid systems exhibiting both hydrocarbon generation and accumulation properties. The criteria used for predicting shale hydrocarbon accumulations include: the transformation ratio (TR) indicating maturity of source rocks, geothermal regime, abnormally high pore pressure (AHPP) and reservoir pressure (AHRP), porosity, and specific densities of adsorbed and free hydrocarbons, with differentiation by fluid type. The values of these parameters, which are used as assessment indicators for identifying promising zones, are derived from a digital model of the studied basin and represented as grids, with each cell assigned a specific parameter value. The threshold values for the TR index, reservoir temperature, porosity and AHRP were determined in accordance with commonly accepted guidelines to differentiate promising and unpromising areas. To identify the most productive zones, the individual maps were created for each criterion, and the regions with the highest degree of overlap among favorable parameters were identified as the most promising areas within the shale succession associated with hydrocarbon accumulations.

Keywords: *South Caspian Basin, shale formations, hydrocarbons, unconventional petroleum systems, porosity*

DOI: *10.17580/em.2026.01.01*

Introduction

The principal distinction of shale hydrocarbon (HC) accumulations formed within unconventional petroleum systems lies in the low quality of their reservoir properties. A conventional petroleum system is characterized by a full set of HC migration-related processes: generation, migration and accumulation. The diversity of HC types arises from variations in the spatial and genetic relationships between source and carrier beds, dominant migration pathways and mechanisms, characteristics of HC traps, and the integrity of sealing rocks [1–3].

Unconventional petroleum systems are distinguished by an incomplete (reduced) sequence of these processes, primarily due to restricted HC migration and accumulation. The most common scenario is formation of an unconventional system as a result of retention of generated hydrocarbons directly within petroleum source rocks (SR).

In the South Caspian Basin (SCB), three unconventional shale petroleum systems can be identified: the diatomaceous suite, the Maikop series, and the Eocene formation. These shale formations have been studied through outcrop analysis, core samples from boreholes, and material expelled from mud volcanoes. The research confirms the shale nature of these units, which represent hybrid systems possessing both generative and accumulative HC properties [4–6].

Prediction criteria for shale hydrocarbon accumulations

The prediction criteria for shale hydrocarbon accumulations were: transformation ratio (TR) of the source rock (SR), geothermal regime, abnormally high pore pressure (AHPP) and reservoir pressure (AHRP), porosity, and the specific densities of adsorbed and free hydrocarbons, with separation by fluid type. The values of these criteria, considered as evaluation parameters for delineating promising areas, are derived from a digital model of the studied basin, and are presented as grids, with each grid cell assigned a specific parameter value. The grid cell spacing is 2 km.

To distinguish between *promising* and *unpromising* zones based on the TR index, reservoir temperature, porosity and AHRP, the threshold values were found in accordance with generally accepted guidelines (**Table 1**).

To identify the most productive zones, maps were generated for each individual criterion. Areas where the maximum number of productive zones overlap indicate the most promising zones within the shale interval associated with hydrocarbon accumulations. Shale content maps were obtained by multiplying the following parameters: TR Index × Reservoir Temperature × Porosity × AHRP × Hydrocarbon Density. Similar calculations were performed separately for free hydrocarbons and for free oil and free gas, as well as for adsorbed hydrocarbons, adsorbed oil and adsorbed gas [7–10].

Table 1. Criteria of hydrocarbon potential of shale accumulations

Criterion	Criterion values	Evaluation	
		Promising zones	Unpromising zones
TR (potential)	> 20%	1 (>20%)	0.4 (<20%)
Reservoir temperature	>110°C	1 (>110°C)	0.4 (<110°C)
Porosity	> 2%	1 (>2%)	0.4 (<2%)
AHRP	>3.5 MPa	1 (>3.5 MPa)	0.4 (<3.5 MPa)
Specific density of free and adsorbed hydrocarbons	> Mean volume×standard deviation×2	1 (>criterion value)	0.4 (<criterion value)

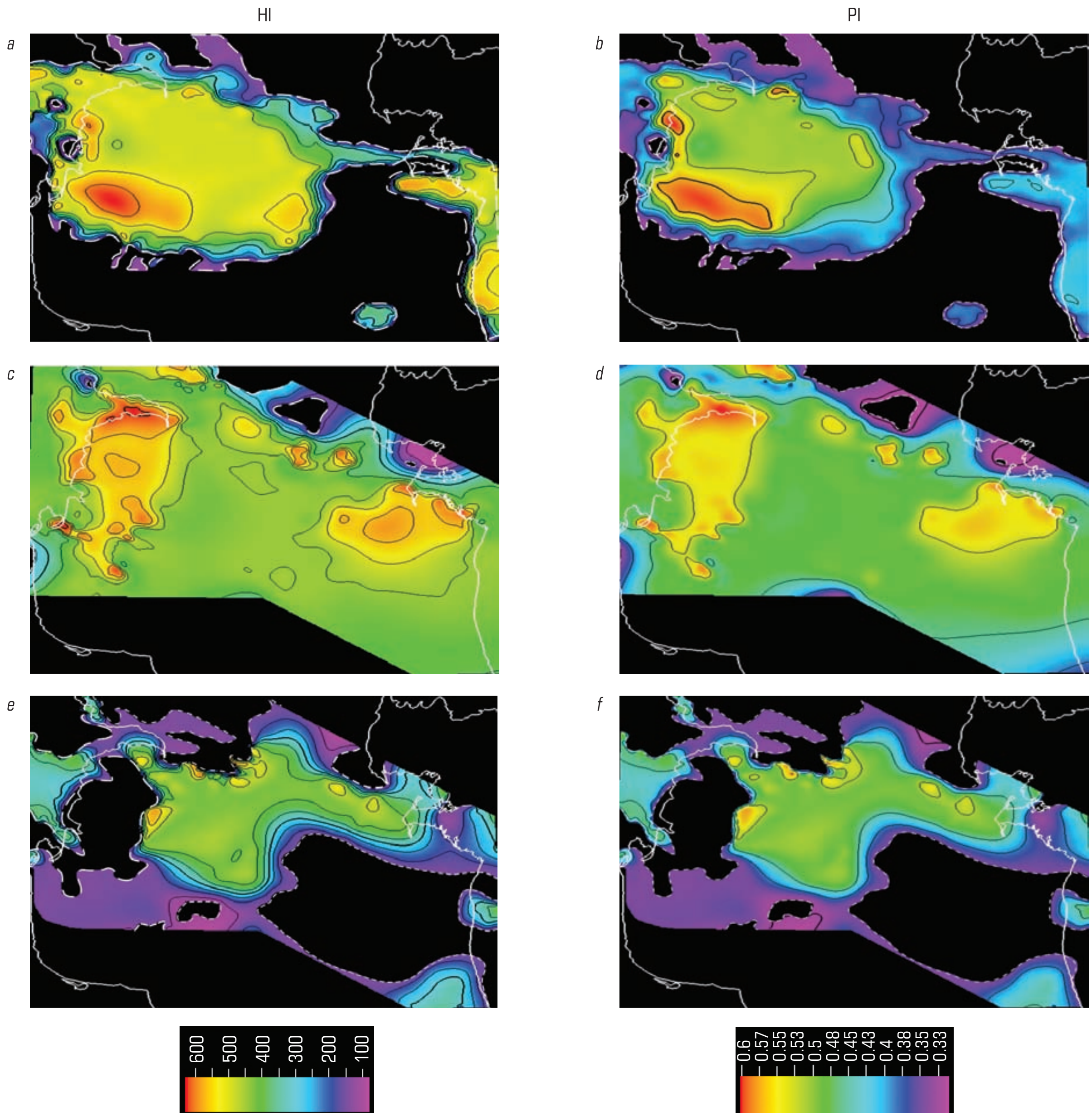

Fig. 1. Maps of pyrolytic parameter distribution (HI and PI) in SCB:
a and *b*—Eocene SR; *c* and *d* —Maikop SR; *e* and *f*—Diatom SR

Transformation ratio of source rock

The transformation ratio (TR) represents the degree to which a source rock has realized its original hydrocarbon generation potential, expressed as a percentage. TR is defined as the ratio of the hydrocarbons already generated to the total potential of the source rock (**Fig. 1**). The formula for calculating TR is as follows [11]:

$$TR = (HI_{initial} - HI) / HI_{initial} \times 1200 / (1200 - HI) \times 100\%,$$

where $HI_{initial}$ is the initial Hydrogen Index (prior to hydrocarbon generation), mg HC/g TOC; HI – is the Hydrogen Index based on pyrolysis data, mg HC/g TOC; 1200 – is the coefficient reflecting the maximum potential hydrocarbon yield per unit mass of organic carbon, mg HC/g TOC.

The PI index is one of the calculated pyrolysis parameters used to assess the current maturity (in a broad sense) of source rocks. Moreover, PI can be used to calibrate basin models by comparing the calculated TR with the measured PI values. In PetroMod, initial values for generative potential are set, and forward modeling is performed; therefore, the Hydrogen Index and TR values are used in this context [12].

Based on the pyrolysis data, TR values were determined for the source rocks of the Diatom, Maikop and Eocene formations (**Table 2**).

Geothermal regime in SCB

The geothermal regime of SCB is one of the most critical factors controlling hydrocarbon generation conditions. To estimate subsurface temperatures at depths uncovered by well thermometry, a method proposed by V. Yu. Kerimov and M. Z. Rachinsky [5] was applied. According

Table 2. Pyrolysis parameters of the Diatom, Maikop and Eocene SR in SCB

SR	TOC	TOC_0	HI	HI_0	PC (GOC)	RC	TR_1	TR_2
Diatom	1.91	2.36	184.46	208.71	0.17	1.74	0.23	23
Maikop	1.25	1.29	139.87	162.84	0.14	1.11	0.26	26
Eocene	1.21	1.24	138.2	160.89	0.12	1.09	0.30	30

TOC—Total Organic Carbon content in rock, wt. %; TOC_0—Initial Total Organic Carbon content in rock, wt. %; HI—Hydrogen Index (by Rock-Eval pyrolysis), mg HC/g TOC; HI_0—Initial Hydrogen Index, mg HC/g TOC; PC (GOC)—Generative Organic Carbon, wt. %; TR_1—Transformation Ratio of organic matter (dimensionless); TR_2—Transformation Ratio of organic matter (percentage)

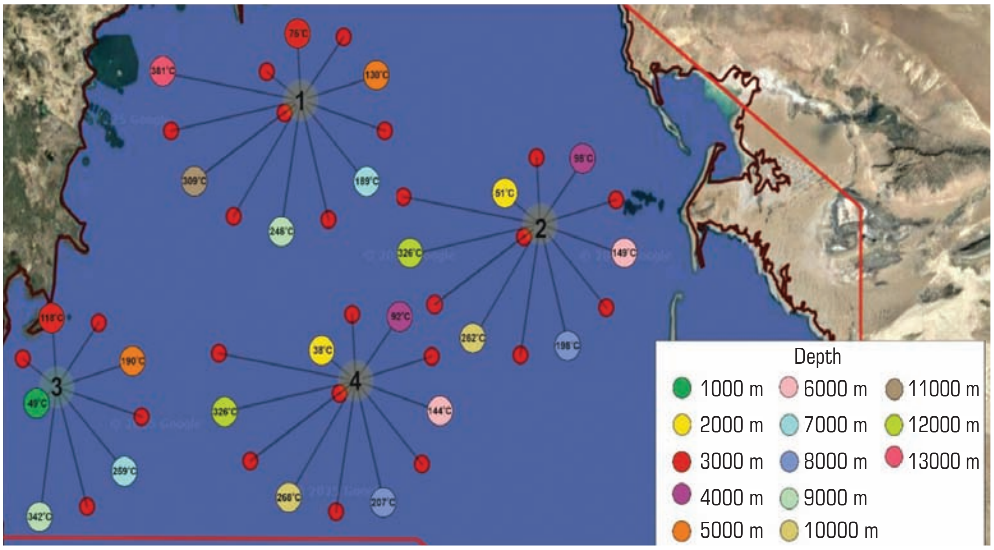

Fig. 2. Geothermal field of SCB (based on well and calculated data)

to this method, temperature prediction at deeper stratigraphic and hypsometric levels is carried out by extrapolating the present-day temperatures at the base of the productive series using standard geothermal gradients, derived from the empirical dependence $t = f(H)$ for the Miocene–Paleogene interval within the actual hypsometric range of its presence in the sedimentary succession. The estimated temperatures at the base of this interval are then used as a starting point for further extrapolation using the reference Mesozoic geothermal gradient down to the top of the crystalline basement. The results of combining measured and calculated well data are presented as maps of temperature distribution for different hypsometric levels (**Fig. 2**).

The geothermal characteristics of the Paleogene–Miocene sediments in SCB are as follows: in the deepest central part of the basin at the base of the complex (Mesozoic surface), within the depth range of 8.7–10.5 km, the calculated temperature values (t_pg-mi) range from 171°C to 231°C. The geothermal gradient varies from 2.17 to 2.27°C/100 m or –19.7 to –22.0°C/km. In the Azerbaijani sector of the basin (depth range 0.5–12 km), the empirical geothermal gradient is described by the function $t\_pg\text{-}mi = 13.9 + 0.0544H^{0.898}$, with a gradient range of –2.59 to –1.87°C/100 m. In the Turkmen sector (depth range 0.5–9 km), the relation is expressed as $t\_pg\text{-}mi = 16.8 + 0.5375H^{0.602}$, with gradients between –2.72 and 0.86°C/100 m [13].

The analysis of the geothermal component of the overall geo-fluid-dynamic field in SCB indicates that the present-day thermal regime of the sedimentary cover is governed by the lithofacies composition of stratigraphic sections in different areas, the degree of tectonic disruption of local structures, and the mobility conditions of thermal groundwater. A significant portion of the heat flux is formed by a convective component—heat transport by migrating fluids, which is controlled by through-flow and injection processes hydraulically linking the lower and upper levels of the basin lithosphere [14–16].

In the Caspian region, particularly in the Lower Kura Depression and Baku Archipelago, this process is significantly slowed due to abnormally low geothermal gradients (1.3–1.7°C/100 m). Here, temperatures at depths of 6000 meters do not exceed 100–110°C. Under such thermal conditions, the formation of subsurface metamorphic brines in SCB would be expected at depths of 20–25 km, where temperatures are estimated to reach 250°C. In the northwestern and northern marginal zones of the basin, including the Shamakhi–Gobustan and Absheron structural belts, geothermal gradients are somewhat higher (2.0–2.2°C/100 m). Therefore, hydrocarbon generation centers in these areas are found at shallower depths compared to the deeply buried axial zones of the basin. There is evidence that hydrocarbon generation in SR of SCB may occur at somewhat lower temperatures due to overpressure in clay-rich formations. In the central part of the basin, where SR are expected at greater depths, the organic matter tends to be more thermally mature [14].

Abnormally High Pore and Reservoir Pressures

A characteristic feature of SCB is the presence of intervals with abnormally high pore pressures (AHPP) and abnormally high reservoir pressures (AHRP) within the Meso-Cenozoic succession. The formation of synsedimentary AHPP in the montmorillonite-rich Paleogene–Miocene clay formations results from two sequential processes. During the first stage (diagenesis to early catagenesis), the dominant factor is the

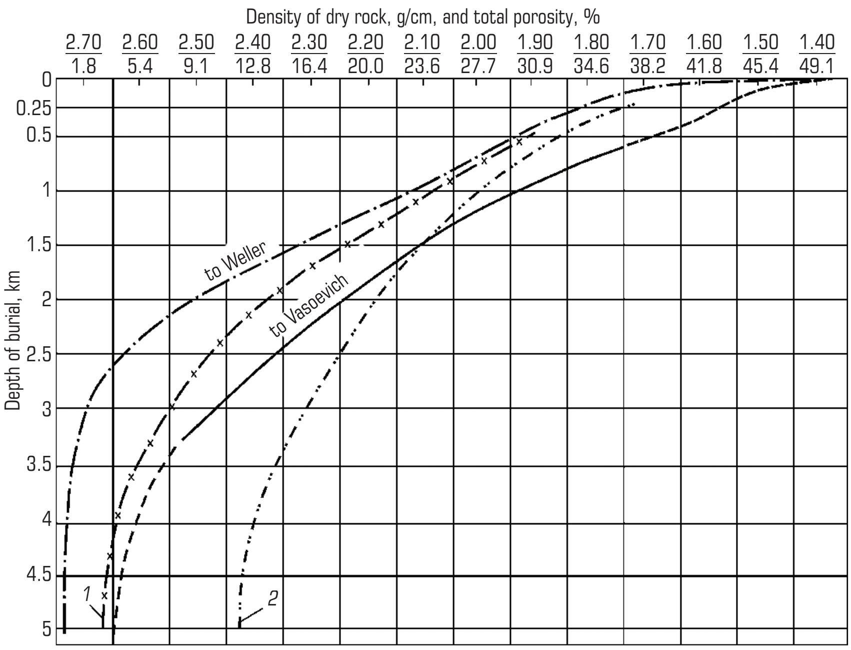

Fig. 3. Relationship of density, porosity and occurrence depth in clay formations:
1—Central Absheron; *2*—Baku Archipelago

and excess pressure arising from the density difference between gas and water.

The Paleogene interval (Paleocene and Eocene deposits) is nearly entirely composed of thick, highly plastic clays with rare, thin and lens-like reservoir interbeds. Indicators of overpressured conditions in these Paleogene clays are evident during drilling: stuck pipe, tight spots, borehole wall collapse, spontaneous rise of the drill string, and borehole ballooning. These phenomena were consistently observed in nearly all parts of the basin where such deposits were penetrated, indicating the widespread regional occurrence of AHPP near lithostatic (overburden) pressure levels. Notably, the roots of most mud volcanoes in the region—which extrude vast quantities of plastic clays—are associated with Paleogene deposits.

The Oligocene–Miocene section (Maikop series, Chokrak horizon, and Diatom suite) has been drilled by numerous deep wells across the Gobustan region, the Absheron Peninsula, several offshore structures of the North Absheron Uplift Zone, the Absheron and Baku Archipelagos, the South Absheron Depression, the Absheron–Pribalkhan Ridge, and the Resht and Gorgan (onshore) Depressions. During drilling operations in the Oligocene–Miocene complex, significantly elevated pore pressures were encountered in clay formations, exceeding hydrostatic pressure. With increasing depths of top and bottomhole intervals, the frequency of overpressured zones rises, complicating drilling and necessitating the use of substantially heavier drilling fluids.

Thus, the spatial analysis of AHPP distribution in the Paleogene–Miocene interval, the intensity of their manifestations, and their correlation with the geological evolution of the basin and its current geothermal regime indicate that the overpressures are synsedimentary in origin and are produced by three primary mechanisms: normal compaction of clays during an immersional subsidence cycle under restricted pore water outflow; subsequent dehydration of montmorillonite under optimal thermodynamic conditions, as indicated by a downward stratigraphic decrease in montmorillonite and a corresponding increase in hydromica content; lateral and vertical tectonic compression during block movement and basement deformation.

gravitational load of overlying sediments, which compresses the trapped interstitial pore water, reducing fluid expulsion and thus decreasing pore space. In the second stage (catagenesis), the primary factor becomes the generation of an excess volume of dehydration ("regenerated") water within the pores of the clay, often accompanied by partial undercompaction of the rock matrix. In some cases, the increase in pore volume in such clays may reach 20–40%.

The South Caspian Basin is characterized by dominant subsiding tectonic movements, resulting in widespread undercompacted and overpressured clays with synsedimentary AHPP across its sedimentary sections. These undercompacted clay-rich rocks play a crucial role in the formation of shale hydrocarbon accumulations. In the Paleogene–Miocene complex, incompetent intervals are widespread within the clayey-shale units, which express ductility, overpressuring, and deformation of strata. The compaction trends of these clay formations are illustrated by the porosity–depth correlations (**Fig. 3**) [15, 16].

The comparison of coeval stratigraphic sections in the Absheron region and the Baku Archipelago in SCB shows that the degree of clay compaction in each of these areas varies significantly depending on the proportion and thickness of permeable and impermeable formations. When reservoir rocks are present within predominantly clay-rich sequences exhibiting abnormally high pore pressure (AHPP), the hydrocarbon potential is primarily determined by the thickness and lateral continuity of permeable intervals. In thicker reservoirs, relatively large accumulations can form within lens-shaped, heterogeneous sand bodies, typically exhibiting scattered hydrocarbon saturation, mostly in the liquid phase (oil). Indeed, the synsedimentary nature of AHPP in highly argillaceous deposits precludes the formation of large gas accumulations with significant, inherently excessive pressures. The presence of such accumulations in formations with synsedimentary AHPP would cause extremely high pressure zones due to a combination of regional AHPP

Porosity and permeability of shale formations in SCB

These parameters are determined based on the lithotype, texture and grain-size distribution of the formations present in the study area (**Fig. 4**) [17].

The diatomaceous shale formation is divided into shale laminae and a ~60 m thick layer of "paper shales" [18]. The Maikop SR shale formation is composed of multilayered pelitic rocks interbedded with shale layers. The Eocene shale formation consists of alternating discrete intervals of shale laminae and organic-rich multilayered pelitic rocks. In the matrix of the studied rocks, pore space is represented by interaggregate or intercrystalline pores, whose morphology was shaped by lithogenesis (depositional environment and subsequent dia- and catagenesis) [18–20]. These kerogen-bearing shale formations include fissile, finely laminated, and foliated argillite-like clays and marls containing various forms of organic matter (OM) at different transformation stages.

Porosity and permeability in clay-rich shale formations are primarily related to the presence and transformation of clay minerals. According to studies by T. T. Klubova, the productive capacity of clay reservoirs is controlled not only by macro-pores but also by the junctions of texturally distinct zones, which represent weakened boundaries. The separation of rocks along these weak zones, as well as fracturing, leads to fragmentation. The formation of reservoir potential in clay rocks occurs during catagenesis, during the generation of HC. The clay rocks become reservoirs at the moment of HC saturation, which forces the rock apart along weak zones and fills them.

Thus, productive capacity of clay reservoirs is related to:

- The specific mineral composition of clay rocks represented by hydromica, silica and OM. Their geochemical interaction results in reduced density, enhanced porosity, and the formation of a rigid but porous silica framework;
- Textural heterogeneity which arises from geochemical interaction between the main rock-forming components. At the interfaces of differing textures, weak zones appear and form the basis of reservoir potential;
- Hydrophobization of clay mineral crystal surfaces, and hence, the entire contact zone between them and other microcomponents via adsorbed OM. This hydrophobization facilitates separation of rock parts during oil saturation, which is critical in clay-hosted reservoirs.

Due to the structure of clay minerals, all reactions between them and OM, including oil-related hydrocarbons, occur on the surfaces of crystals of clayey mineral characterized by layered structures.

The results confirm previous assumptions [19] about the role of OM transformation in porosity, particularly the appearance and development of kerogen-related porosity. As OM is consumed during catagenesis to generate hydrocarbons and non-HC products, its mass decreases, though residual concentrations remain at each stage. In dense immature kerogen, organic pores begin to form, and by the end of the main oil generation phase, these pores form a connected system that provides space for newly generated oil HCs. Organic pores within the kerogen texture significantly contribute to the reservoir space within productive formations [21–23].

Kerogen pore development is proportional to the volume of generated and expelled HC during primary migration [24, 25]. Y. Han, N. Mahlstedt, and B. Horsfield have shown that organic porosity plays a key role in hydrocarbon adsorption, especially of high-molecular-weight compounds. Based on pyrolysis data, organic porosity of SR was quantitatively assessed, and the impact of pore space on hydrocarbon generation and retention was interpreted.

C. J. Modica and Scott G. Lapierre [26], as well as F. Chen, Sh. Lu, and X. Ding [27], proposed simplified equations to estimate organic porosity in SR:

$$PO_1 = TOC_0 \cdot GOC \cdot TR \cdot k \cdot D_1/D_2 \text{ [28]}; \quad (1)$$

$$PO_2 = [(TOC_0 \cdot HI_0 \cdot TR \cdot k \cdot D_1/D_2)] / 1000 \text{ [27]}, \quad (2)$$

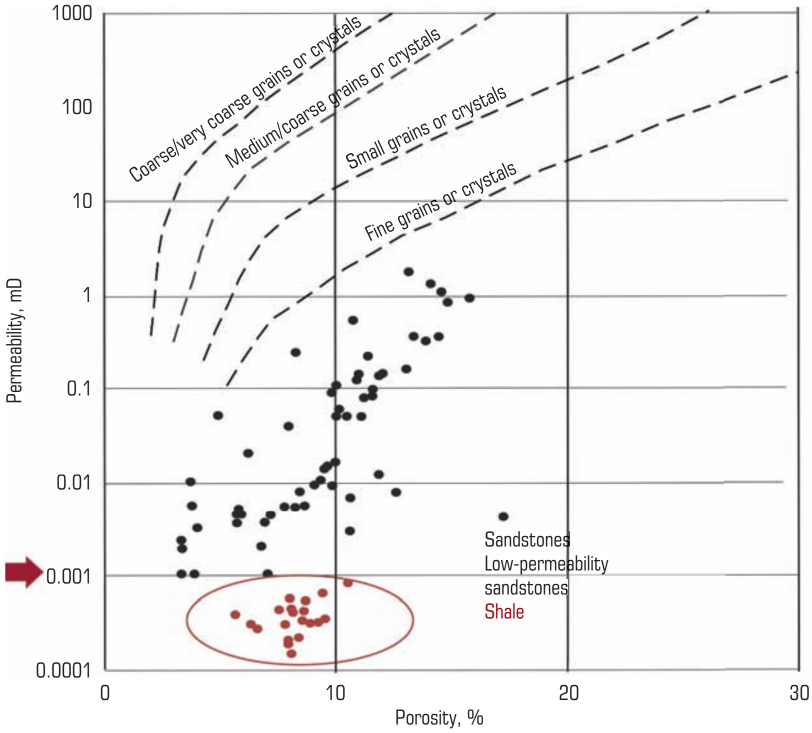

Fig. 4. Porosity–permeability diagrams of different types of rocks

Table 3. Pyrolysis-based results from well samples for SR in SCB

SR	HI^1	HI_0^2	PC (GOC)^3	PO^4_{1-1}	PO^5_{1-2}	PO^6_{2-1}	P^7_{O2-2}
Diatom	184.46	208.71	0.17	0.29	29	0.35	35
Maikop	139.87	162.84	0.14	0.18	18	0.22	22
Eocene	138.2	160.89	0.12	0.22	22	0.28	28

HI^1—Hydrogen Index (based on Rock-Eval), mg HC/g TOC; HI_0^2—Original Hydrogen Index, mg HC/g TOC; PC (GOC)^3—Generative Organic Carbon, %; PO^4_{1-1}—organic porosity, fractional units (based on Eq. 1); PO^5_{1-2}—organic porosity, % (based on Eq. 1); PO^6_{2-1}—organic porosity, fractional units (based on Eq. 2); PO^7_{2-2}—organic porosity, % (based on Eq. 2)

where $GOC = HI_0 / 1200$ is the organic carbon component; 1200 is the maximum hydrogen index value per unit of organic carbon; $HI_0 = HI + HI(Tmax - 435)/30$ is the initial hydrogen index; $TOC_0 = TOC / (1 - GOC)$ is the initial total organic carbon; $TR = (HI_0 - HI) / HI_0$ is the transformation ratio; $GOC_0 = TOC_0 \cdot GOC$ is the initial labile organic carbon content; $D_1 = 8.0$ g/cm^3 is the rock density; $D_2 = 1.2$ g/cm^3 is the kerogen density; $k = 0.95 / 0.85 = 1.118$ is the correction factor accounting for ~5% kerogen loss during diagenesis and assuming that labile carbon represents 95% of kerogen mass [29]; samples with $Tmax \le 435$°C were considered thermally immature and excluded from processing.

The average calculated organic porosity values are: $PO_1 = 0.29\%$ and $PO_2 = 0.35\%$ for the diatomaceous SR; $PO_1 = 0.18\%$ and $PO_2 = 0.22\%$ for the Maikop SR; $PO_1 = 0.22\%$ and $PO_2 = 0.28\%$ for the Eocene SR (**Table 3**). These values may represent up to 20% of total porosity [27].

The hydrocarbon source diatomaceous, Maikop and Eocene clayey-shale formations in SCB are composed of multilayered pelitic rocks—clays, marls, argillites, and true shales—that host various forms of OM. Distinguished by their textural characteristics from other pelitic rocks, clay shales exhibit the ability to split into thin laminae.

The Miocene sequence is mainly composed of thin-bedded clays with occasional interlayers of dolomite, calcite, and siderite. These clays are saturated with oil and bitumen. The laminated clays of the Miocene sequence are likely both hydrocarbon-generating and hydrocarbon-bearing.

Laminated clays are also widespread in the thin-bedded clay formations of the Maikop Series in the South Caspian region. Hydrocarbon-bearing laminated clays are also found in the Maikop Formation deposits of the Pre-Caspian–Guba region. In this area, oil-filled lenses are observed within the laminated clays.

Studies of clayey rocks indicate that hydrocarbon-bearing formations may include not only layered and texturally heterogeneous clays but also dense, homogeneous rocks characterized by micro- and macrofracturing. These include fractured argillites and tuffaceous argillites, primarily encountered in older Paleogene-Jurassic formations. For instance, microfractured dense argillites are found in Upper Cretaceous deposits of the Middle Kura Depression (Ganja district, Yevlakh-Agjabedi trough, and between the Kura and Gabyrri rivers. These argillites have undergone intense catagenesis (mesocatagenesis), are dehydrated and lack sufficient sealing capacity.

Studies of deep hydrocarbon potential in SCB [1–3, 29, 30] have shown that at depths exceeding 8–9 km, regionally distributed complexes of abnormally undercompacted sedimentary rocks exist, featuring favorable thermobaric and structural-lithological conditions for hydrocarbon accumulation and preservation. It is well known that the interval of moderate catagenesis in clay sediments coincides with the main oil and gas generation window. A key feature of this interval is the progressive transformation of montmorillonite into illite with increasing depth, which completes at the base of the moderate catagenesis zone.

Density of adsorbed and free hydrocarbons

Hydrocarbon accumulations in shale formations are composed of both free hydrocarbons and those retained through sorption. Organic porosity on the surface of kerogen significantly influences the adsorption of generated hydrocarbons.

The fundamental mechanism governing the interaction of petroleum hydrocarbons and dissolved organic compounds with sedimentary rock minerals (primarily clays) is the adsorption of organic molecules onto the mineral surface, particularly at defect sites where a deficit of positive charges exists. The adsorption capacity of clay minerals depends on several factors, with surface forces playing a key role—these increase with specific surface area, i.e., higher mineral dispersion.

During catagenesis, desorption of generated hydrocarbons occurs as vapor bubbles form, creating pits and deforming the kerogen surface. The porous surface of kerogen exhibits high adsorption activity and retains the generated hydrocarbons. The development of kerogen pore space is proportional to the volume of hydrocarbons generated and expelled during primary migration. The type of kerogen also affects adsorption capacity [31]. The surface area of organic pores becomes significant and greatly impacts the amount of gas stored in free versus adsorbed condition [28, 31, 32].

Adsorption increases the concentration of a substance at the phase boundary [3] and is governed by the following principles:

- Adsorption is localized (occurs at active sites), in this case on the surface of organic pores in kerogen;
- Adsorption occurs not over the entire surface but only at active centers—protrusions or cavities on the adsorbent surface;
- Each active center can interact with only one adsorbate molecule;
- Adsorption is in dynamic equilibrium with desorption.

Adsorption can occur from either the liquid or gas phase gas–solid, liquid–solid, gas–liquid, or liquid–liquid interfaces.

Results

Assessment of hydrocarbon potential of the Eocene shale petroleum system

According to the methodology described above, the maps were generated for each of the hydrocarbon potential assessment criteria, including TR of SR, AHPP, porosity, reservoir temperature, and specific densities of both free and adsorbed hydrocarbons within the Eocene shale unit. These maps are presented in **Fig. 5.**

Figure 5*a* displays the map of TR values. The promising areas with TR values exceeding 20% are marked in a semi-transparent gray shade; the rest of the region with TR below 20% is considered unpromising. The highlighted area of favorable values encompasses almost the entire SCB.

The promising zones for the AHPP criterion (above 3.5 MPa) are found throughout most of the study area, except for the Absheron–Pribalkhan uplift system and the northwestern portion of the region (Fig. 5*b*). For the criterion of porosity, the threshold was set at the values above 2%. The promising zone based on this criterion also covers nearly the entire SCB (Fig. 5*c*). The preferred reservoir temperatures for shale hydrocarbon accumulations are above 110°C. The map in Fig. 5*d* shows that the promising area based on this criterion occupies nearly the entire SCB.

Figures 5*e* and 5*f* present the maps of the specific densities of free and adsorbed hydrocarbons, respectively. The most promising zones according to these parameters are also delineated. Free hydrocarbons are primarily concentrated in the central part of SCB, with smaller accumulations on the Turkmen shelf. Adsorbed hydrocarbons are predominantly distributed along the coastal areas and onshore zones of Azerbaijan and Turkmenistan.

Overall, the main volumes of both free and adsorbed hydrocarbons are concentrated primarily onshore in Azerbaijan and Turkmenistan, as well as in the central part of SCB. A notably large area of free gas accumulation is observed on the Azerbaijani shelf.

The total volumes of free hydrocarbons (oil + gas) are estimated at 440 Mt, while the total volumes of adsorbed hydrocarbons (oil + gas) amount to 486 Mt.

Assessment of hydrocarbon potential of the Maikop shale source rock

The maps for each of the evaluation criteria for the hydrocarbon potential of the Maikop shale source rock are presented in **Fig. 6**. Figure 6*a* shows the TR; promising areas with TR values greater than 20% are highlighted with a semi-transparent gray shade. These areas cover nearly the entire SCB.

According to the criterion of AHPP exceeding 3.5 MPa, the promising zones are traced across most of the study area, with the exception of the Absheron–Pribalkhan uplift and the northwestern part of the region (Fig. 6*b*).

For the porosity criterion, a threshold value of more than 2% was used. The promising areas by this parameter include the northwestern

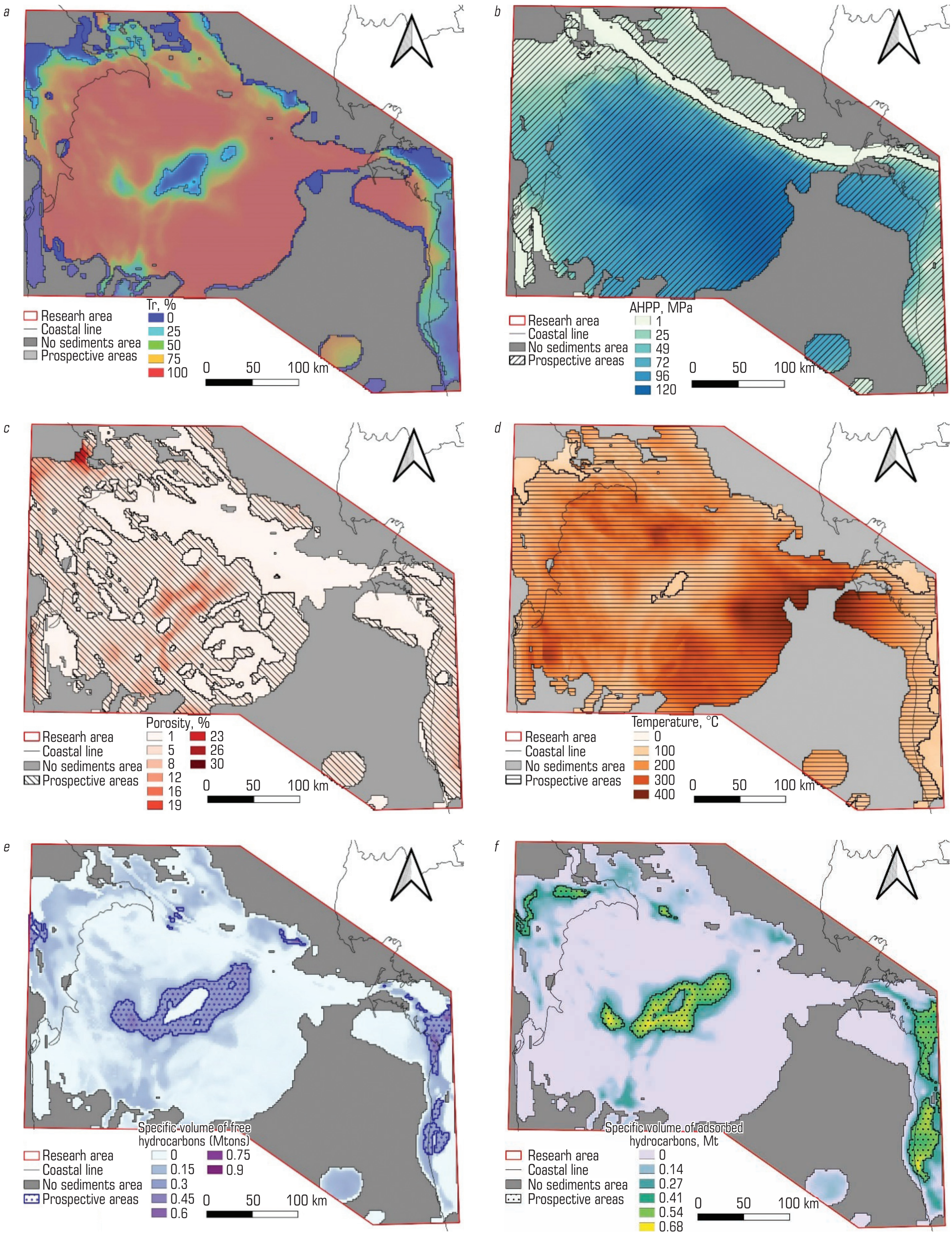

Fig. 5. Distribution maps of parameters for the Eocene shale unit:

a—TR index, %; *b*—AHPP (abnormally high pore pressure), MPa; *c*—porosity, %; *d*—reservoir temperature, °C; *e*—specific volume of free hydrocarbons, Mt of oil equivalent; *f*—specific volume of adsorbed hydrocarbons, Mt

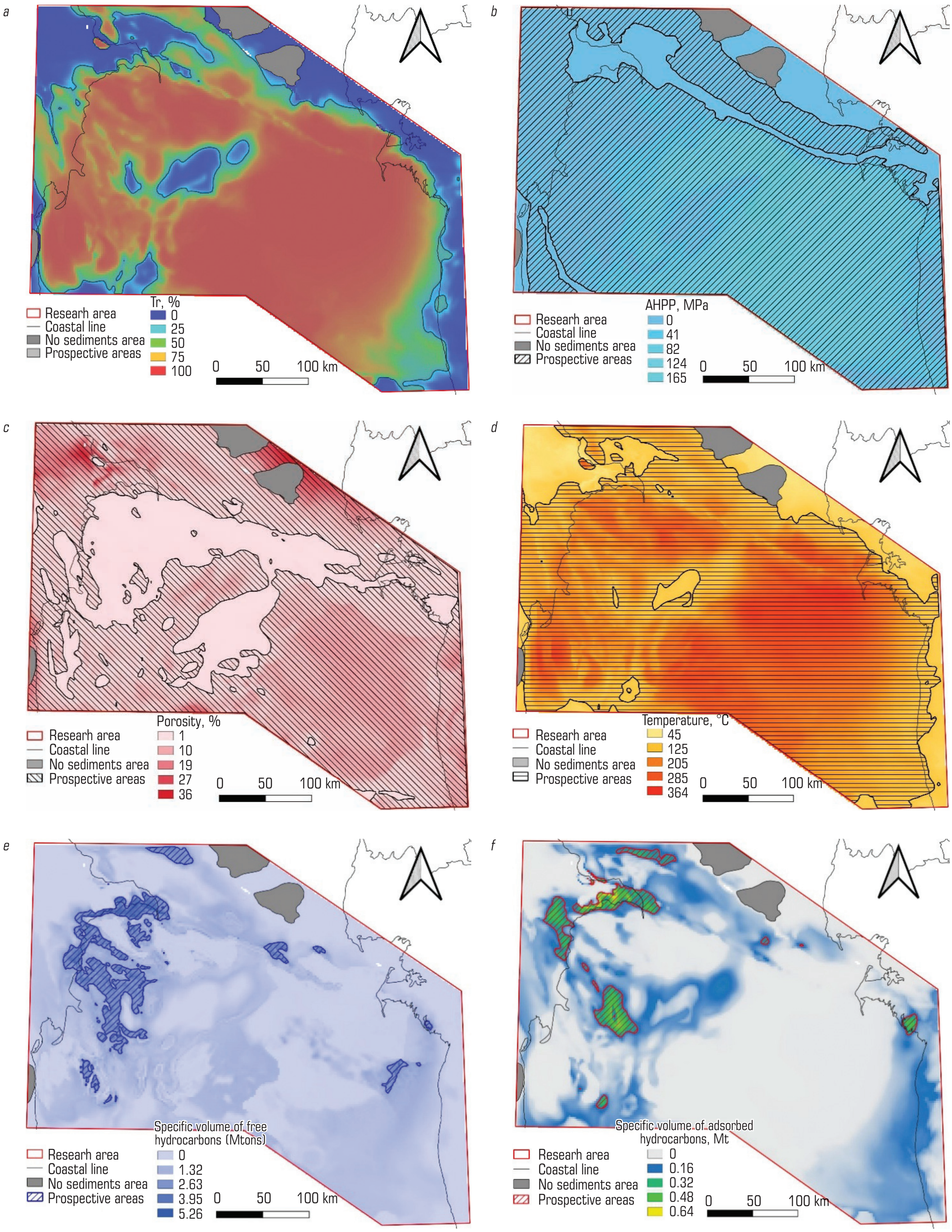

Fig. 6. Distribution maps of parameters for the Maikop shale formation:
a—Transformation Ratio (TR), %; *b*—Abnormally High Formation Pressure (AHFP), MPa; *c*—porosity, %; *d*—reservoir temperature, °C; *e*—specific volume of free hydrocarbons, Mt; *f*—specific volume of adsorbed hydrocarbons, Mt

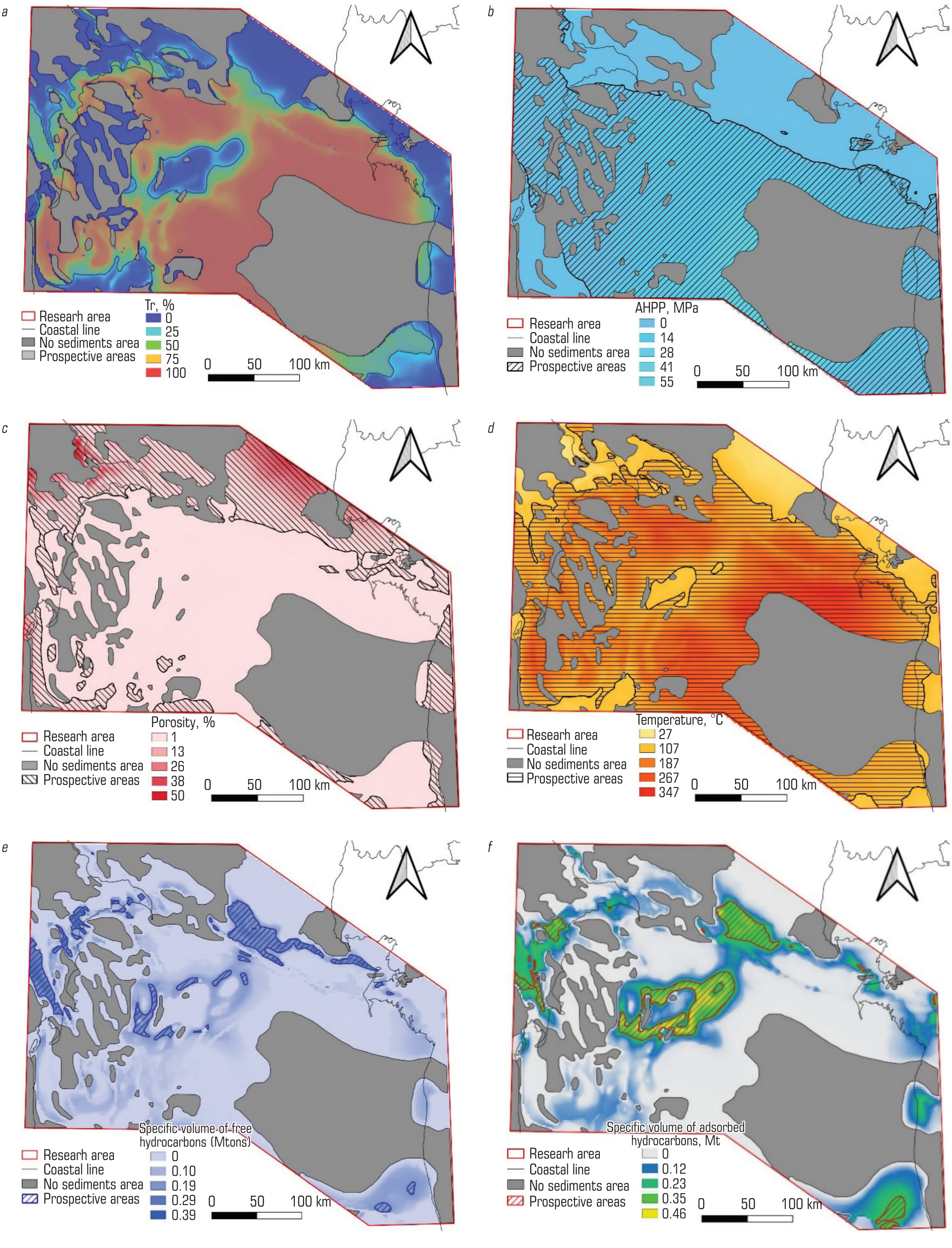

Fig. 7. Maps of parameter distribution for the diatomaceous shale unit:

a—TR index, %; *b*—abnormally high formation pressure, MPa; *c*—porosity, %; *d*—formation temperature, °C; *e*—specific volume of free hydrocarbons, Mt; *f*—specific volume of adsorbed hydrocarbons, Mt

Table 4. Volumes of free and adsorbed hydrocarbons in shale petroleum systems of SCB

Type of HC	Volume of the Eocene unconventional petroleum system (million tons of oil equivalent)	Volume of the Maikop unconventional petroleum system (million tons of oil equivalent)	Volume of the Diatom unconventional petroleum system (million tons of oil equivalent)	TOTAL (million tons of oil equivalent)
Free hydrocarbons	440	2126	284	2850
Free oil	442	1637	264	2343
Free gas	147	1260	60	1467
Adsorbed Hydrocarbons	486	104	309	899
Adsorbed oil	403	82	257	742
Adsorbed gas	67	22	47	136
TOTAL	**1986**	**5231**	**1 221**	**8 438**

part of the Absheron–Pribalkhan uplift, the Kura Depression, the entire Turkmen structural terrace, and a significant part of the deep-water basin of the SCB (Fig. 6*c*).

The preferred reservoir temperatures for the formation of shale hydrocarbon accumulations are above 110 °C. According to the map (Fig. 6*d*), such conditions are observed throughout almost the entire SCB.

The maps of the specific volumes of free (Fig. 6*e*) and adsorbed (Fig. 6*f*) hydrocarbons, differentiated by fluid type, highlight the most promising areas. According to these maps:

• Free hydrocarbons (oil and gas) are primarily concentrated in the offshore area of the Azerbaijani shelf and, to a lesser extent, on the Turkmen shelf.

• Adsorbed hydrocarbons are mainly concentrated in the coastal zone and onshore areas of Azerbaijan.

Thus, the main volumes of free and adsorbed hydrocarbons are concentrated in the offshore and nearshore areas of Azerbaijan. Additionally, a significant accumulation of free gas is identified on the Turkmen shelf.

The total volumes of free hydrocarbons (oil + gas) are estimated at 2126 Mt, while the total volumes of adsorbed hydrocarbons (oil + gas) amount to 104 Mts.

Assessment of hydrocarbon potential of the diatomaceous shale petroleum system

The maps corresponding to each evaluation criterion for the hydrocarbon potential of the diatomaceous shale petroleum system are presented in **Fig. 7**. Figure 7*a* shows the TR map. The promising areas with TR values exceeding 20% are highlighted with a semi-transparent gray shade. The favorable area extends across nearly the entire SCB.

The promising zones based on the criterion of abnormally high pore pressure (over 3.5 MPa) are observed throughout most of the study region, with the exception of the Absheron–Pribalkhan uplift system and the northwestern sector of the basin (Fig. 7*b*).

For delineating favorable areas based on porosity, a threshold value above 2% was applied. The favorable zones according to this criterion encompass much of the coastal area of Azerbaijan, the Absheron–Pribalkhan uplift system, and selected parts along the basin's periphery (Fig. 7*c*).

The optimal formation temperature for shale hydrocarbon accumulations is considered to exceed 110 °C. The map in Fig. 7*d* indicates that almost the entire SCB meets this temperature criterion.

Figures 7*e* and 7*f* display maps of specific volumes of free and adsorbed hydrocarbons, respectively, with differentiation by fluid type. The most favorable areas under each parameter are highlighted.

The analysis of these maps indicates that free hydrocarbons (oil and gas) are mainly concentrated in the central part of SCB, and to a lesser extent, on the Turkmen shelf. Adsorbed hydrocarbons are predominantly located in the onshore and nearshore zones of Azerbaijan and Turkmenistan.

The principal accumulations of both free and adsorbed hydrocarbons are concentrated onshore in Azerbaijan and Turkmenistan, as well as in the central part of the basin. A notably large area of free gas occurrence is identified on the Azerbaijan shelf.

The total volume of free hydrocarbons (oil + gas) is estimated at 284 Mt, while the total volume of adsorbed hydrocarbons (oil + gas) amounts to 309 Mt.

Conclusions

The conducted research confirms the shale nature of the diatom suite, Maikop series and Eocene deposits of the South Caspian Basin. These SR form hybrid petroleum systems, which not only generate but also accumulate HC, thus constituting self-contained shale petroleum systems. The spatial boundaries of such systems coincide with the extent of mature SR intervals, which serve simultaneously as both the source and the reservoir.

Three shale petroleum systems have been identified in SCB: the diatom shale petroleum system, the Oligocene–Miocene shale petroleum system and the Eocene shale petroleum system.

These systems represent unconventional, hybrid petroleum systems.

The assessment of shale HC accumulations was based on the following criteria: TR of SR, geothermal regime, AHPP and AHRP, porosity, specific densities of adsorbed and free hydrocarbons with fluid-type differentiation.

The values of these parameters—used to delineate promising areas—were derived from a digital basin model and presented as gridded datasets, with each cell containing a calculated parameter value.

To distinguish promising from unpromising zones, the threshold values were defined for the following indicators: TR index, reservoir temperature, porosity and AHFP. Based on these thresholds, maps were constructed for each individual criterion. Zones of overlapping favorable values across multiple criteria were interpreted as the most productive and promising areas within shale intervals, where HC accumulations are likely to be present.

The total estimated volumes of free and adsorbed hydrocarbons within the shale petroleum systems of the SCB amount to 8.438 billion tons of oil equivalent (**Table 4**).

References

1. Kalmykov A. G., Karpov Yu. A., Topchiy M. S. et al. The effect of catagenetic maturity on the formation of reservoirs with organic porosity in the Bazhenov formation and peculiarities of their extension. *Georesources*. 2019. Vol. 21, No. 2. pp. 159–171.
2. Stupakova A. V., Kalmykov G. A., Fadeeva N. P. et al. On the estimation of shale-oil resources and reserves. *Moscow University Geology Bulletin*. 2015. Vol. 70, No. 3. pp. 183–190.
3. Dolson J. Understanding Oil and Gas Shows and Seals in the Search for Hydrocarbons. Coconut Grove, FL, USA : Springer Cham, 2016. 486 p.
4. Petroleum Geology Atlas. Caspian Sea Region. Ed. by Ya. P. Malovitsky, B. V. Senin, F. T. Lysell. Norway, Oslo : PGS Reservoir AS, PA Soyuzmorgeo, 1997. Vol. I, II, III.
5. Kerimov V. Y., Rachinsky M. Z. Fluid Dynamics of Oil and Gas Reservoirs. New Jersey : Wiley, 2015. 617 p.
6. Gadgiev A. N. Paleogeographic setting of the pre-Pliocene time and the role of the Paleo-Volga in the formation of the sedimentary basins of the Eastern Paratethys. *Structure and Petroleum Potential of the Basins of the Inland Seas*. Moscow : IGiRGI, 1989. pp. 65–69.
7. Katz M. E., Wright J. D., Miller K. G. et al. Biological overprint of the geological carbon cycle. *Marine Geology*. 2005. No. 217. pp. 323–338.
8. Malovitsky Ya. P., Senin B. V. Black Sea-Caspian Region - Comparative Petroleum Geology of Deep-Water Basins of different Age. *62nd EAGE Conference & Exhibition*. 2000. DOI: 10.3997/2214-4609-pdb.28.P10
9. Kerimov V. Yu., Senin B. V., Serikova U. S. et al. Assessment of the conditions of formation and distribution of structural, lithological, stratigraphic and combined traps in the Black Sea – Caspian region. *ANAS Transactions, Earth Sciences*. 2023. No. 1. pp. 81–99.
10. Abrams M. A., Narimanov A. A. Geochemical evaluation of hydrocarbons and their potential sources in the western South Caspian depression, Republic of Azerbaijan. *Marine and Petroleum Geology*. 1997. Vol. 14, Iss. 4. pp. 451–468.
11. Pelet R. Evaluation quantitative des produits formés lors de l'évolution géochimique de la matiĕre organique. *Revue de l'Institut Français du Pétrole*. 1985. Vol. 40, No. 5. pp. 551–562.
12. Veber V. V., Kotseruba L. A. Conditions of bituminous content in the Bazhenov Formation of Western Siberia. *Russian Oil And Gas Geology*. 1979. No. 9. pp. 15–19.
13. Kerimov V. Yu., Guliyev I. S., Javadova A. S. et al. Shale oil and gas systems of the south caspian depression. *ANAS Transactions, Earth Sciences*. 2024. No. 2. DOI: 10.33677/ggianas20240200131
14. Kerimov V. Yu., Mustaev R. N. Lithology and geochemical characterization of low-permeability shale strata: A-case-study of Khadum Formation in Ciscaucasia. *Gornyi Zhurnal*. 2021. No. 7. pp. 28–33.
15. Kerimov V. Yu., Shilov G. Ya., Mustaev R. N., Dmitrievskiy S. S. Thermobaric conditions of hydrocarbons accumulations formation in the low-permeability oil reservoirs of Khadum suite of the pre-caucasus. *Oil industry*. 2016. No. 2. pp. 8–11.
16. Atlas of paleogeographic maps: Eurasian shelves in the Mesozoic and Cenozoic. Ed. by M. N. Alekseeva. GIN USSR Academy of Sciences, Robertson Group. 1992. Vol. 1, Vol. 2.
17. Hartmann D. J., Beaumont E. A., Coalson E. Predicting Sandstone Reservoir System Quality and Example of Petrophysical Evaluation. *Search and Discovery*. 2000. ID 40005.
18. Prischepa O. M., Averyanova O. Yu. Contributions to the terminology of hydrocarbons bearing shale formations – unconventional sources of oil and gas. *Neftegazovaya geologiya. Teoriya i praktika*. 2013. Vol. 8, No. 3. DOI: 10.17353/2070-5379/27_2013
19. Levin L. E., Senin B. V. Deep structure and dynamics of sedimentary basins in the Caspian Region. *Doklady Earth Sciences*. 2003. Vol. 388, No. 1. pp. 12–15.
20. Senin B. V., Kerimov V. Yu., Mustaev R. N., Leonchik M. I. Structural-Geodynamic Systems of the Basement of the Black Sea–Caspian Sea Region: Evolution in the Late Paleozoic–Cenozoic. *Geotectonics* 2022. No. 1. pp. 27–50.
21. Aghayeva V., Sachsenhofer R. F., Van Baak C. G. C., Bechtel A., Hoyle T. M. et al. New geochemical insights into Cenozoic source rocks in Azerbaijan: Implications for petroleum systems in the South Caspian region. *Journal of Petroleum Geology*. 2021. Vol. 44, No. 3. pp. 349–384.
22. Sondergeld C. H., Newsham K. E., Comisky J. T. et al. Petrophysical Considerations in Evaluating and Producing Shale Gas Resources. *SPE Unconventional Gas Conference*. Pittsburgh, *Pennsylvania, USA*. 2010. pp. 1–34.
23. Alizade A. A., Guliev I. S., Mamedov P. Z. et al. Productive Series of Azerbaijan : in 2 volumes. Moscow : Nedra, 2018. Vol. 1. 305 p., Vol. 2. 236 p.
24. Mann U., Hantschel T., Schaefer R. G. et al. Petroleum migration: Mechanisms, Pathways, efficiencies and numerical simulations. *Petroleum and Basin Evolution*. 1997. pp. 403–520.
25. Pepper A. S., Corvi P. J. Simple kinetic models of petroleum formation. Part III: Modelling an open system. *Marine and Petroleum Geology*. 1995. Vol. 12, Iss. 4. pp. 417–452.
26. Modica C. J., Lapierre S. G. 2012. Estimation of kerogen porosity in source rocks as a function of thermal transformation: Example from the Mowry Shale in the Powder River Basin of Wyoming. *AAPG bulletin*. 2012. Vol. 96, No. 1. pp. 87–108.
27. Chen F., Lu Sh., Ding X. Organoporosity Evaluation of Shale: A Case Study of the Lower Siluian Longmaxi Shale in Southeast Chongqing, China. *The Scientific World Journal*. 2014. Vol. 2014, No. 8. ID 893520.
28. Dakhnova M. V., Mozhegova S. V., Nazarova E. S., Paizanskaya I. L. Evaluation of reserves of shale oil using geochemical parameters. *Russian Oil and Gas Geology*. 2015. No. 4. pp. 55–61.
29. Zou Caineng, Yang Zhi, Zhang Guosheng et al. Conventional and unconventional petroleum "orderly accumulation": Concept and practical significance. *Petroleum Exploration and Development*. 2014. Vol. 41, Iss. 1. pp. 14–30.
30. Ottman J., Bohacs K. Conventional reservoirs hold keys to the 'Un's. *AAPG Explorer*. 2014.
31. Guliev I. S., Klyatsko N. V., Mamedova S. A., Suleymanova S. V. Oil/gas-producing and reservoir properties of sedimentary deposits in the South Caspian Basin. *Lithology and Mineral Resources*. 1992. No. 2. pp. 110–119.
32. Glumov I. F., Malovitskiy Ya. P., Novikov A. A., Senin B. V. Regional Geology and Oil and Gas Content of Caspian Sea. Moscow : Nedra, 2004. 342 p.